Neuropsychopharmacology (2017) 42, 1272–1283

www.neuropsychopharmacology.org

GABAb Receptor Mediates Opposing Adaptations of GABA Release From Two Types of Prefrontal Interneurons After Observational Fear

Lei Liu[1], Wataru Ito[1] and Alexei Morozov*[,1,2,3]

[1]Virginia Tech Carilion Research Institute, Roanoke, VA, USA; [2]School of Biomedical Engineering and Sciences, Virginia Tech, Blacksburg, VA, USA; [3]Department of Psychiatry and Behavioral Medicine, Virginia Tech Carilion School of Medicine, Roanoke, VA, USA

The observational fear (OF) paradigm in rodents, in which the subject is exposed to a distressed conspecific, elicits contextual fear learning and enhances future passive avoidance learning, which may model certain behavioral traits resulting from traumatic experiences in humans. As these behaviors affected by the OF require dorso-medial prefrontal cortex (dmPFC), we searched for synaptic adaptations in dmPFC resulting from OF in mice by recording synaptic responses in dmPFC layer V pyramidal neurons elicited by repeated 5 Hz electrical stimulation of dmPFC layer I or by optogenetic stimulation of specific interneurons *ex vivo* 1 day after OF. OF increased depression of inhibitory postsynaptic currents (IPSCs) along IPSC trains evoked by the 5 Hz electrical stimulation, but, surprisingly, decreased depression of dendritic IPSCs isolated after blocking GABAa receptor on the soma. Subsequent optogenetic analyses revealed increased depression of IPSCs originating from perisomatically projecting parvalbumin interneurons (PV-IPSCs), but decreased depression of IPSCs from dendritically projecting somatostatin cells (SOM-IPSCs). These changes were no longer detectable in the presence of a GABAb receptor antagonist CGP52432. Meanwhile, OF decreased the sensitivity of SOM-IPSCs, but not PV-IPSCs to a GABAb receptor agonist baclofen. Thus, OF causes opposing changes in GABAb receptor mediated suppression of GABA release from PV-positive and SOM-positive interneurons. Such adaptations may alter dmPFC connectivity with brain areas that target its deep *vs* superficial layers and thereby contribute to the behavioral consequences of the aversive experiences.
Neuropsychopharmacology (2017) **42,** 1272–1283; doi:10.1038/npp.2016.273; published online 4 January 2017

INTRODUCTION

Traumatic experiences, even those without physical pain, are a risk factor for mental disorders (Cougle *et al*, 2009; Resnick *et al*, 1995), but how they alter relevant neuronal circuits remains unknown. The observational fear (OF) paradigm in rodent models certain components of socially induced trauma without physical pain or physical discomfort. The subject observer animal is exposed once to a conspecific demonstrator receiving electrical footshocks and emitting distress signals via multiple modalities. The distress signals act as an unconditional stimulus and lead to memorization of the associated cues and context (Chen *et al*, 2009; Jeon *et al*, 2010; Yusufishaq and Rosenkranz, 2013). We have recently shown that OF also enhances future learning in the passive avoidance (PA) task and causes the formation of silent synapses in the input from the dorso-medial prefrontal cortex (dmPFC) to the basolateral amygdala (Ito *et al*, 2015).

*Correspondence: Dr A Morozov, Virginia Tech Carilion Research Institute, Virginia Tech, 2 Riverside Circle, Roanoke, VA 24016, USA, Tel: 540-526-2021, Fax: 540-985-3373, E-mail: alexeim@vtc.vt.edu.
Received 26 February 2016; revised 29 November 2016; accepted 2 December 2016; accepted article preview online 7 December 2016

As dmPFC is involved in Pavlovian conditioning (Malin *et al*, 2007; Malin and McGaugh, 2006) and undergoes synaptic remodeling during contextual fear learning (Bero *et al*, 2014), we hypothesized that OF also elicits plastic changes within dmPFC, which could potentially underlie the fear learning during OF, or the stronger PA learning in the future. We searched for changes at synapses that target pyramidal cells (PCs) in dmPFC layer V. These cells belong to dmPFC major output neurons. They innervate multiple targets including the cortex, amygdala, striatum, thalamus, brainstem nuclei and spinal cord (Gabbott *et al*, 2005; Hirai *et al*, 2012; Shepherd, 2013). As their apical dendrites extend towards the superficial layer of dmPFC, the layer V PC are positioned to integrate information from all cortical layers by receiving inputs from local neurons and remote projections from all over the brain (Ramaswamy and Markram, 2015). Our analysis suggests that OF redistributes flow of that information by reorganizing inhibitory control of inputs to the layer V neurons by two types of interneurons that are distinguished by expression of parvalbumin (PV) and somatostatin (SOM).

MATERIALS AND METHODS

Animals

C57BL/6N males were crossed with 129SvEv females to obtain wild-type mice or with homozygous 129SvEv interneuron-specific Cre-driver females for interneuron-specific expression of ChR2. Male pups were housed two littermates per cage (Allentown, NJ) since weaning as detailed in Ito *et al* (2015). All experiments were approved by Virginia Tech IACUC and followed the NIH Guide for the Care and Use of Laboratory Animals.

Viral Injection Surgery

ChR2-AAV pseudo-type 1 virus containing Cre-activated *ChR2* gene was prepared by the University of North Carolina Gene Therapy Vector Core (Chapel Hill, NC) using a plasmid pAAV-*EF1a*-double floxed-*hChR2 (H134R)-EYFP* (Addgene 20298). Heterozygous male *Pvalb*$^{tm1(cre)Arbr}$ (Hippenmeyer *et al*, 2005) or *Sst*$^{tm2.1(cre)Zjh}$ (Taniguchi *et al*, 2011) transgenic mice were injected bilaterally with 0.5 µl of the viral solution (10^8 viral particles) per hemisphere in dmPFC at 1.3 mm anterior, 0.4 mm lateral from the bregma, and 1.3 mm ventral from brain surface, as described (Ito *et al*, 2015). Previous studies have demonstrated specific expression of ChR2 in SOM-INs and PV interneurons (PV-INs) of dmPFC using these lines and AAV vector (Kim *et al*, 2016; Sohal *et al*, 2009).

Behavior

OF procedure (Jeon *et al*, 2010) was performed at age of p60–75 during light phase of the day cycle in a fear conditioning chamber (Med Associates, St Albans, VT), divided into two unequal compartments by a transparent Plexiglas wall with 7 mm diameter holes, spaced at 2 cm interval, to allow auditory and olfactory cues and whisker-to-whisker interaction. In the larger $26 \times 20 \times 26$ cm (depth, width, height) compartment, a stainless-steel rod floor was covered with a white plastic sheet. In the smaller $26 \times 9 \times 26$ cm compartment, the rod floor was exposed. Cagemates observer and demonstrator were placed in the larger and the smaller compartments, respectively. After 5 min acclimation, 24 footshocks (1 mA, 2 s, every 10 s) were delivered to the demonstrator. In the control procedure, demonstrators did not receive footshocks. The observers (OF or controls) were returned to the home cage and housed alone until preparation of brain slices for physiology on the next day.

Electrophysiology

Next day after OF training, under deep isoflurane anesthesia, animals were decapitated. Brains were immersed in an ice-cooled cutting solution containing (in mM) 110 Choline Cl, 2.5 KCl, 1.2 NaH_2PO_4, 2.5 $NaHCO_3$, 20 glucose, 0.5 $CaCl_2$, and 5 $MgSO_4$, and bubbled with a 95% O_2/5% CO_2. Coronal dmPFC slices, 300 µm thick, were cut using DSK Microslicer (Ted Pella, Redding, CA) and incubated in solution containing (in mM) 120 NaCl, 3.3 KCl, 1.0 NaH_2PO_4, 25 $NaHCO_3$, 10 glucose, 0.5 $CaCl_2$, and 5 $MgSO_4$, bubbled with 95% O_2/5% CO_2 gas mixture at room temperature for at least 1 h before recording. Recording chamber was superfused at 2 ml/min with ACSF equilibrated with 95% O_2/5% CO_2 and containing 120 NaCl, 3.3 KCl, 1.0 NaH_2PO_4, 25 $NaHCO_3$, 10 glucose, 2 $CaCl_2$, and 1 $MgCl_2$. Whole-cell recordings were obtained at 30 ± 1 °C with Multiclamp 700B amplifier and Digidata 1440 A (Molecular Device, Sunnyvale, CA). Putative layer V principle neurons in dmPFC were identified by their pyramidal morphology under the Dodt gradient contrast optics (custom made) at 850 nm LED illumination (Thorlabs, Newton, NJ) and were recorded using 4–6 MΩ pipettes filled with K+-based internal solution (in mM): 130 K-gluconate, 1 $MgCl_2$, 10 HEPES, 0.2 EGTA, 2 ATP-Mg, 0.1 GTP-Na pH 7.3, or Cs+-based internal solution (in mM): 120 Cs-methanesulfonate, 5 NaCl, 1 $MgCl_2$, 10 HEPES, 0.2 EGTA, 2 ATP-Mg, 0.1 GTP-Na, and 5 QX314 pH 7.3, osmolarity 285 Osm. Series resistance (Rs) was 10–20 MΩ and monitored throughout experiments. Data were not included in the analysis if Rs changed > 20%. All membrane potentials were corrected for the junction potential of 12 mV. For electrical stimulation of layer I, 0.1 ms pulses of current, 30–80 µA range, were delivered via a 6 MΩ pipette filled with ASCF. The current was adjusted to obtain postsynaptic responses as described in results. Light pulses (470 nm, 1 ms) were generated using an LED lamp (Thorlabs) and a custom LED driver based on MOSFET, and were delivered through a ×40 objective lens (Olympus, Center Valley, PA) at 0.3–2.5 mW, calibrated by a photodiode power sensor (Thorlabs) at the tip of the lens. In some experiments, to block somatic components of evoked inhibitory postsynaptic currents (IPSCs), picrotoxin (1 mM) was puffed on the soma of recorded neurons via a 1–2 MΩ pipette, positioned at ~50 µm from the target, by three 300 ms puffs driven by 1 psi air pressure (PDES-02DX, NPI Electronic GmbH, Tamm, Germany). The spread of picrotoxin towards apical dendrites was minimized by directing the puffing and the flow of ACSF from superficial to deep layers of dmPFC. In most experiments, data from each cell were obtained from 19 to 20 stimuli sweeps separated by 20 s intervals. Baclofen and CGP52432 were from Tocris (Bristol, UK) and remaining chemicals were from Sigma-Aldrich (St Louis, MO).

Data Analysis

Statistical analyses were performed using GraphPad Prism (GraphPad Software, La Jolla, CA) and StatView (SAS Institute, Cary, NC). Charge transfer (voltage clamp) or EPSP time integral (current clamp) were measured as the area under the trace during a 45 ms time window starting 1.5 ms after the stimulus artifact or stimulus onset for electrical and blue light stimulation, respectively. Differences were tested using the two-tailed unpaired, paired and one sample *t*-test, repeated measure, one- or two-way ANOVA, and Bonferroni multiple comparisons as appropriate, and deemed significant with $p < 0.05$.

RESULTS

OF Training Increases Excitability of L5 PCs and Causes EPSP Facilitation During Repetitive Stimuli

To study effects of OF on glutamatergic transmission, dmPFC layer I was stimulated with 5 Hz trains of five

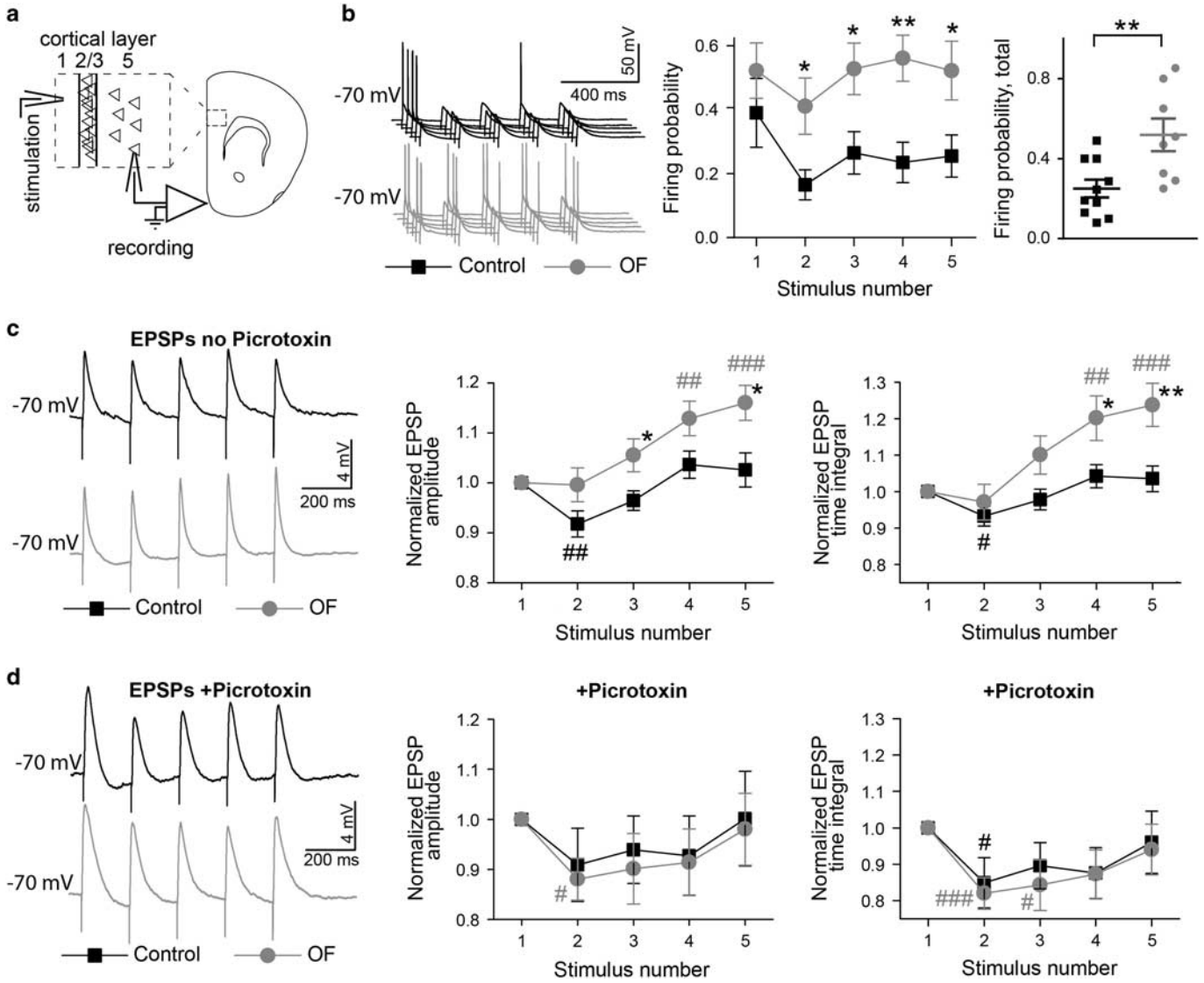

Figure 1 Observational fear training (OF) increases excitability of dorso-medial prefrontal cortex (dmPFC) layer V principal neurons and enhances facilitation of EPSPs evoked by a 5 Hz train of electrical stimuli. (a) Experimental scheme. Stimulation of dmPFC layer 1 and recording from principal neurons in layer V are illustrated. (b) Left: examples of responses to AP threshold stimulation with 5 Hz train in control (upper, black) and OF group (lower, gray). Right; firing probabilities at each stimulus and across five stimuli (total), control (black): 10 cells/3 mice, OF (gray): 9 cells/3 mice. (c) Left: examples of EPSPs evoked by AP subthreshold stimulation, averages of 5 sweeps are shown. Right: EPSP amplitudes and time integrals normalized to the values of the first EPSP, control: 18 cells/3 mice, OF: 22 cells/3 mice. (d) Same experiment as in c, but in the presence of picrotoxin (100 μM), control: 9 cells/3 mice, OF: 9 cells/3 mice. OF *vs* control: $^{*}p<0.05$ and $^{**}p<0.01$; intragroup comparison to the first pulse responses: $^{\#}p<0.01$, $^{\#\#}p<0.01$, and $^{\#\#\#}p<0.001$. Error bars represent s.e.m.

electrical pulses and evoked postsynaptic responses were recorded from layer V PCs (Figure 1a) maintained at −70 mV in current clamp mode. To examine the susceptibility of neurons to generating action potentials in response to the repeated stimulation, stimulus intensity was set to elicit EPSPs of about 20 mV by the first pulse in the train, which brought membrane potential to −50 mV, near the action potential threshold. In response to the first pulse in the train, neurons from the OF group mice showed a tendency, although nonsignificant ($p>0.05$), of having a higher probability of firing action potential than neurons from the control group mice. The probability became significantly higher during the second through the fifth pulses of the train ($p<0.01$, collapsed data for stimuli 2–5) (Figure 1b). We next examined the EPSP dynamics along the train of stimuli adjusted to obtain the first EPSP at 4 to 10 mV, which was below the threshold for the action potential. In the control group, the amplitude and time integral of the second EPSP were significantly lower than those of the first EPSP (amplitude: $p<0.01$, time integral: $p<0.05$), whereas the values for the third to fifth EPSPs were the same ($p>0.05$). In contrast, in the OF group, the second EPSP did not differ from the first one ($p>0.05$), whereas the values for the fourth and fifth EPSPs were significantly higher (amplitude and time integral, fourth: $p<0.01$; fifth: $p<0.001$). As a result, the amplitudes of the third ($p<0.05$) and fifth ($p<0.05$) EPSPs and the time integrals of the fifth ($p<0.05$) and fifth ($p<0.01$) EPSPs were higher in the OF

than in control group (Figure 1c). Including GABAa receptor blocker picrotoxin (100 μM) in the bath prevented the facilitation of the fourth and fifth EPSP in the OF group ($p > 0.05$, amplitudes and time integrals compared to the values for the first EPSP) and abolished the differences between OF and control groups in the third through fifth EPSPs ($p > 0.05$) (Figure 1d), suggesting that the OF effects on EPSPs resulted from changes in GABAergic transmission.

OF Training Enhances Depression of IPSCs Recorded from the Soma

Evoked IPSCs were elicited in L5 PCs, voltage clamped at 0 mV, using the same electrode placement and stimulus pattern as in Figure 1, except the stimulus intensity, was adjusted to obtain the first IPSC within 400 to 1200 pA range. Both the IPSC amplitudes and charge transfer decreased along the train in all cells (amplitude: control, $F(4,20) = 53.2$, $p < 0.001$; OF, $F(4,19) = 190$, $p < 0.0001$; charge transfer: control, $F(4,20) = 164$, $p < 0.001$; OF, $F(4,19) = 294$, $p < 0.0001$, repeated measure ANOVA) with greatest decreases occurring between the first and second IPSCs. The IPSC depression was stronger in OF group than in controls (behavioral treatment*amplitude interaction: $F(4,39) = 5.9$, $p < 0.001$; behavioral treatment*charge transfer interaction $F(4,39) = 4.5$, $p < 0.01$), resulting in lower values for the second through fifth IPSCs in OF group (amplitude: $p < 0.01$ or < 0.001; charge: $p < 0.05$ or < 0.01) (Figure 2a). As GABAb auto-receptor contributes to IPSC depression in the neocortex (Fukuda *et al*, 1993; Kobayashi *et al*, 2012), we repeated the experiment in the presence of GABAb receptor (GABAbR) blocker CGP52432 in the bath (10 μM). CGP52432 significantly attenuated the IPSC depression along the train in OF group (CGP52432*IPSC amplitude interaction: $F(4,33) = 14.6$, $p < 0.0001$; CGP52432*IPSC charge interaction $F(4,33) = 25.2$, $p < 0.0001$), thereby eliminating the differences between the control and OF groups in IPSC dynamics (behavioral treatment*amplitude interaction: $F(4,28) = 1.7$, $p > 0.05$; behavioral treatment*charge transfer interaction $F(4,28) = 1.5$, $p > 0.05$), and in the second through fifth IPSCs' amplitudes and charge transfers ($p > 0.05$) (Figure 2b), which suggests that the effects of OF on IPSC dynamics are mediated by changes in a GABAbR-dependent process.

CGP52432 and Evoked Excitation

To determine how GABAbR regulates the evoked action potentials and EPSPs, the same experiments as in Figures 1b and c were performed first in the absence and then after 10 min perfusion with 10 μM CGP52432 (Figure 3). In the absence of CGP52432, the OF group showed a higher probability of total firing ($p < 0.01$) than the controls, reproducing the findings on Figure 1b. Bath application of CGP52432 increased the firing probabilities in both groups during the entire train and upon stimuli 2 through 5 ($p < 0.05$) (Figure 3b), thereby eliminating the differences between the groups. Two-way repeated measure ANOVA showed significant interaction between behavioral treatment and CGP52432 for total firing probability ($F(1,15) = 8.7$,

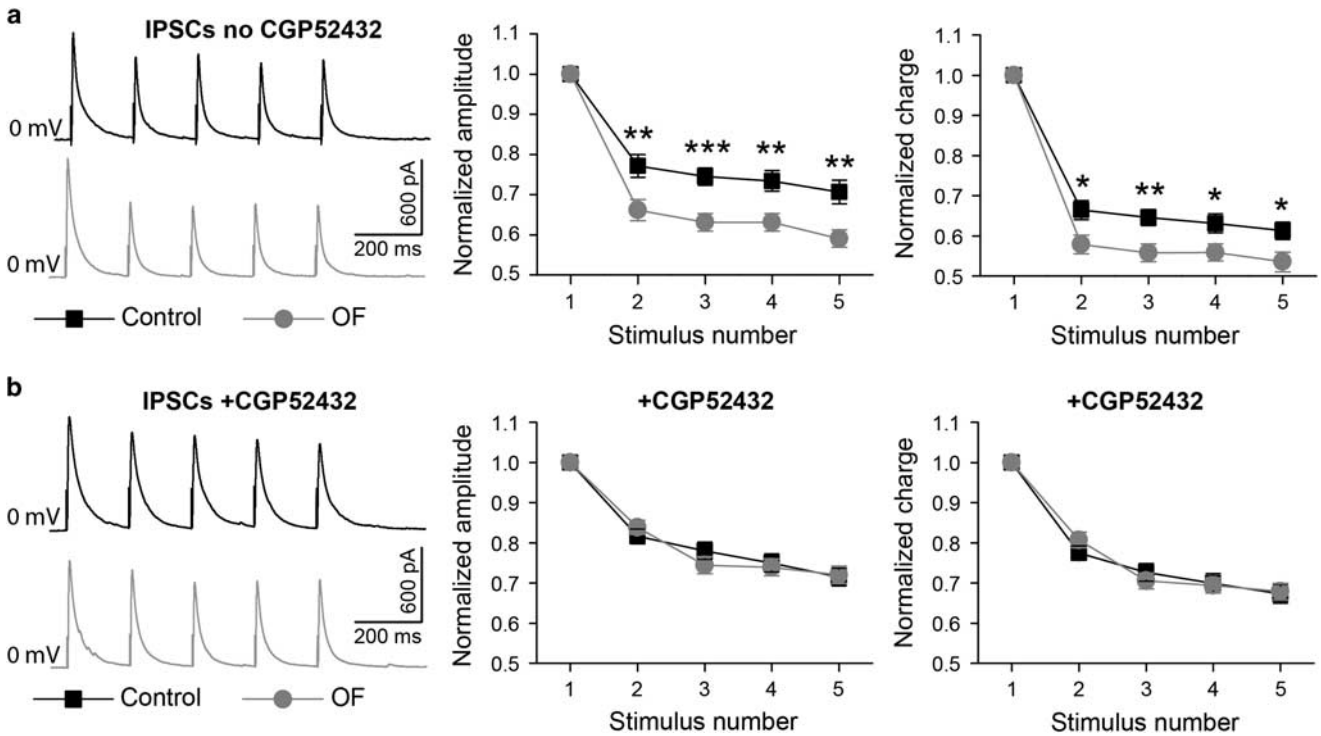

Figure 2 Observational fear training (OF) enhances depression of somatic inhibitory postsynaptic currents (IPSCs). (a) Left: examples of IPSCs evoked in L5 pyramidal cells (PCs) held at 0 mV by 5 Hz train of electrical pulses delivered in L1, averages of five sweeps are shown. Right: IPSC amplitudes and charge transfers normalized to the values of the first IPSC, control: 21 cells/3 mice; OF: 20 cells/3 mice. (b). Same experiment as in a, in the presence of CGP52432 (10 μM), control: 15 cells/3 mice; OF: 15 cells/3 mice. Black and gray colors represent control and OF groups, respectively. OF *vs* control: $*p < 0.05$, $**p < 0.01$, and $***p < 0.001$. Error bars represent SEM.

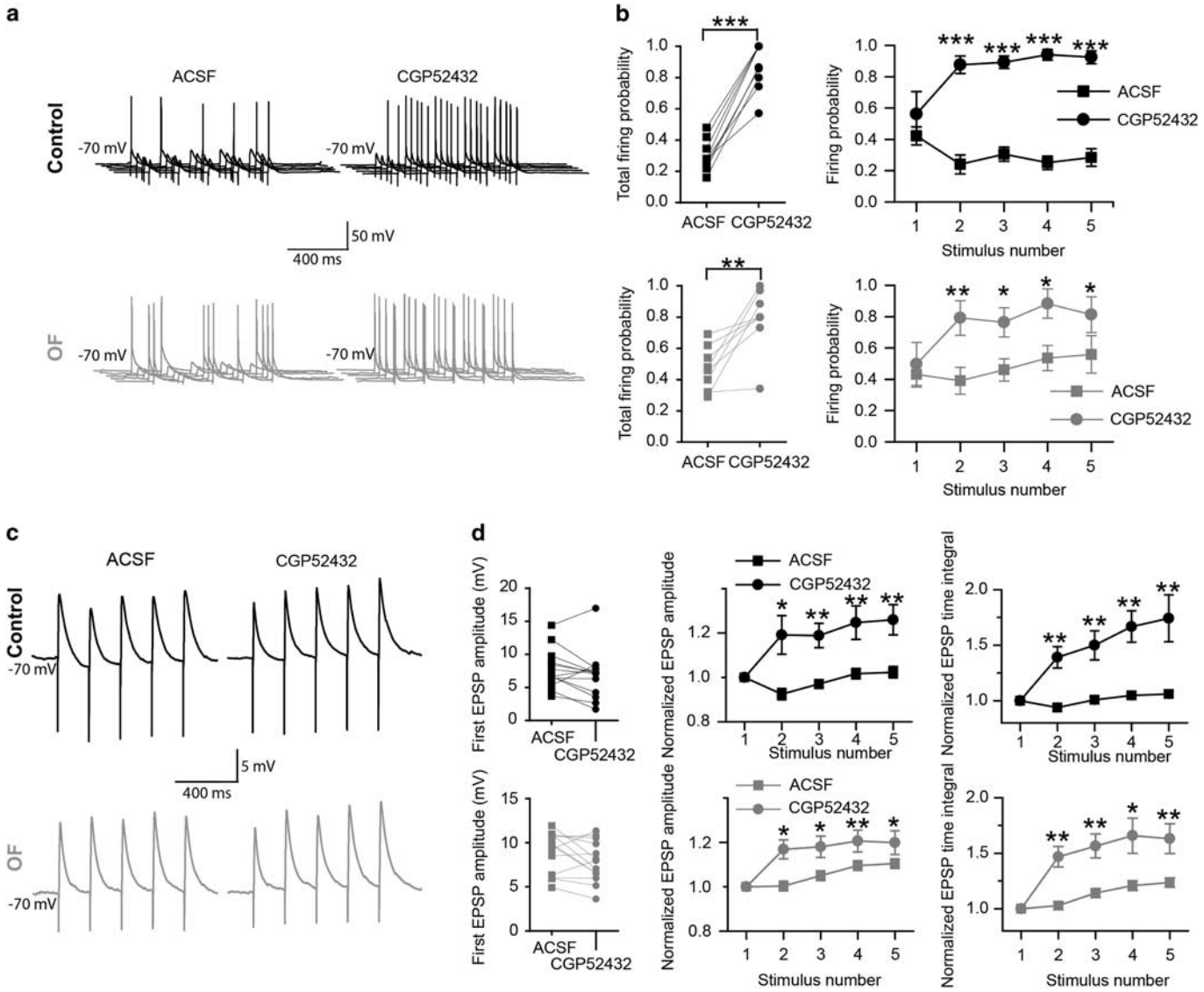

Figure 3 Effects of CGP52432 on evoked excitation. (a) Examples of responses to AP threshold stimulation with 5 Hz train in control (upper) and observational fear (OF) group (lower) before (left, ACSF), and after (right, CGP52432) perfusion with CGP52432. (b) Right: firing probabilities during the entire train (left: data for individual cells) and upon each stimulus in control (upper): nine cells/three mice and OF (lower): eight cells/three mice. (c) Left: examples of EPSPs evoked by AP subthreshold stimulation in control (upper) and OF group (lower) in the same cells before (left, ACSF) and after (right, CGP52432) perfusion with CGP52432. Averages of five sweeps are shown. (d) Left: Amplitudes of the first EPSPs in the train before and after perfusion with CGP52432, lines connect data points representing the same cells. Right: EPSP amplitudes and time integrals normalized to the values of the first EPSP, before and after perfusion with CGP52432; control: 13 cells/3 mice, OF: 13 cells/3 mice. ASCF *vs* CGP52432: $*p<0.05$, $**p<0.01$, and $***p<0.001$. Black and gray colors represent control and OF groups, respectively. Error bars represent SEM.

$p=0.01$) and for firing probabilities upon stimuli 3 ($F(1,15)=6.5$, $p=0.02$), 4 ($F(1,15)=10.4$, $p=0.006$) and 5 ($F(1,15)=11.3$, $p=0.004$). It indicated that the enhancing effect of CGP52432 was weaker in the OF group, likely due to the higher initial firing in the absence of CGP52432. In the subthreshold EPSP experiments, CGP52432 did not change the amplitudes of the first EPSP significantly despite of tendencies to decreases, but enabled facilitation between the first and second EPSPs in both groups (EPSP amplitudes, $p<0.05$; EPSP time integral, $p<0.001$, paired *t*-test) (Figure 3d), which eliminated the differences in EPSC dynamics between the groups described in Figure 1c.

OF Training Attenuates IPSC Depression at Distal Dendrites

Because of the dendritic filtering and poor space clamp at distal dendrites, the outward currents recorded in the soma represent the IPSCs originating mainly from the soma and proximal dendrites (Williams and Mitchell, 2008). To enrich recording for IPSCs originating from distal dendrites, we suppressed GABAa receptor on the soma and proximal dendrites by puffing picrotoxin on the soma of the recorded neuron (Figure 4a). Picrotoxin continued to inhibit GABAa receptor after puffing was over, as indicated by a significant reduction in frequencies (normalized frequency: $p<0.0001$, comparison to 100% baseline, one sample *t*-test) and

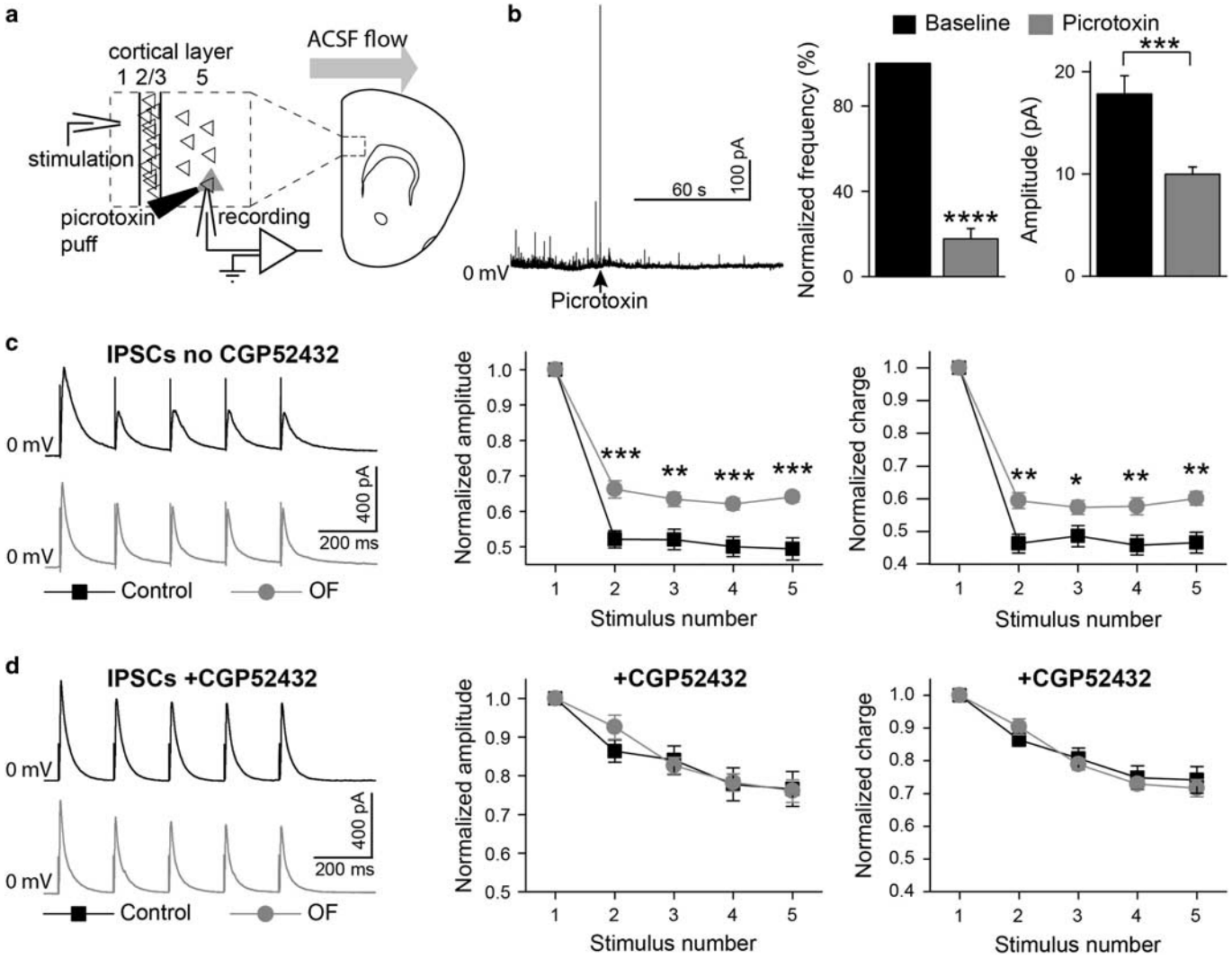

Figure 4 Observational fear training (OF) attenuates depression of dendritic inhibitory postsynaptic currents (IPSCs). (a) Experimental scheme. Stimulation of dmPFC layer I, voltage-clamp recording from the layer V principal neuron held at 0 mV and puffing picrotoxin on soma of the recorded neuron are illustrated. Directions of puffing and ASCF flow are shown. (b). Picrotoxin puff on soma eliminated above 80% of spontaneous IPSCs (sIPSCs) and decreased sIPSC amplitude. Left: an example of sIPSC recorded before and after a somatic puff of picrotoxin. Right: summary data for sIPSCs detected within 1 min before (Baseline) and after (Picrotoxin) puff of picrotoxin (1 mM): sIPSC frequency normalized to the baseline value and absolute amplitude. Data were merged from control and OF groups, six cells/three mice each, as picrotoxin effects were same between the groups. (c) Left: examples of IPSCs evoked by 5 Hz train of electrical pulses, averages of five sweeps are shown. Right: IPSC amplitudes and charge transfers normalized to the values of the first IPSC, control: 11 cells/3 mice, OF: 12 cells/3 mice. (d) Same experiment as in c, in the presence of CGP52432 (10 μM), control: 15 cells/3 mice, OF: 15 cells/3 mice. Black and gray colors represent control and OF groups, respectively. Baseline *vs* Picrotoxin, or OF *vs* control: $*p<0.05$, $**p<0.01$, $***p<0.001$, and $****p<0.0001$. Error bars represent SEM.

amplitudes ($p=0.001$, unpaired *t*-test) of spontaneous IPSC (Figure 4b). In picrotoxin-puffed neurons, evoked IPSCs were depressed along the train in both control and OF groups (amplitude: control, $F(4,10)=208$, $p<0.0001$; OF, $F(4,11)=176$, $p<0.0001$; charge transfer: control, $F(4,10)=224$, $p<0.0001$; OF, $F(4,11)=214$, $p<0.0001$, repeated measure ANOVA), mainly between the first and second IPSCs, resulting in higher normalized amplitudes and charge transfers for the second through fifth IPSCs in OF group (amplitude: $p<0.01$ or <0.001; charge: $p<0.05$ or <0.01) (Figure 4c). Surprisingly, in contrast to the experiment without puffing picrotoxin (Figure 2a), OF attenuated the depression of IPSC along the train (behavioral treatment*amplitude interaction: $F(4,21)=9.5$, $p<0.0001$; behavioral treatment*charge transfer interaction $F(4,21)=7.7$, $p<0.0001$). CGP52432 significantly attenuated the IPSC depression along the train in both the control and OF groups (control, CGP52432*IPSC amplitude interaction: $F(4,24)=37.7$, $p<0.0001$; CGP52432*IPSC charge transfer interaction $F(4,24)=38.0$, $p<0.0001$; OF, CGP52432*IPSC amplitude interaction: $F(4,25)=15.2$, $p<0.0001$; and CGP52432*IPSC charge transfer interaction $F(4,25)=21.8$, $p<0.0001$), and abolished the differences between the control and OF groups in IPSC dynamics (behavioral treatment*IPSC amplitude interaction: $F(4,28)=1.7$, $p>0.05$; behavioral treatment*IPSC charge transfer interaction $F(4,28)=1.5$, $p>0.05$), and in the second through fifth IPSCs' amplitudes and charge transfers ($p>0.05$)

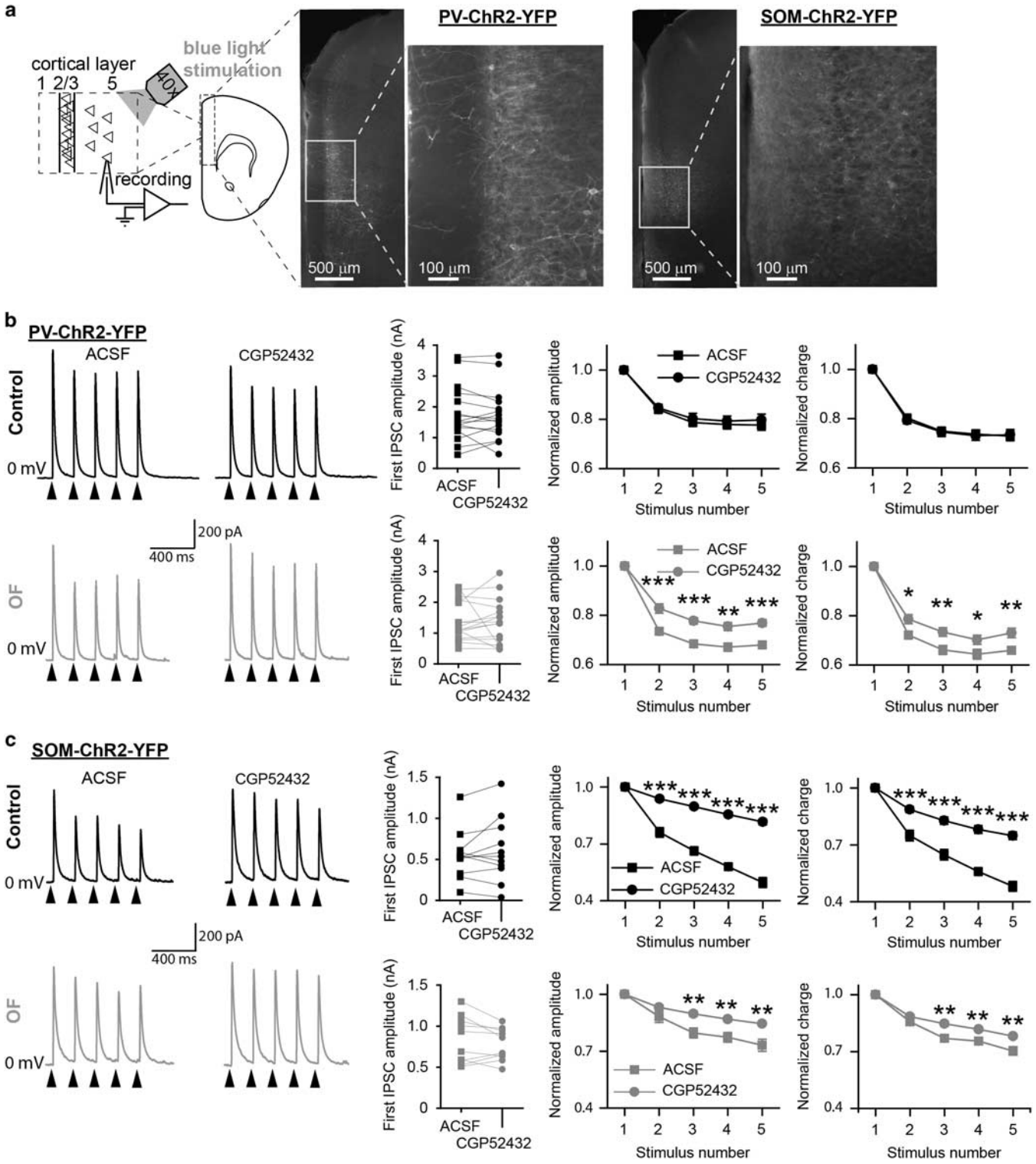

Figure 5 Observational fear training (OF) enhances depression of inhibitory postsynaptic currents (IPSCs) originating from parvalbumin (PV)-positive interneurons but suppresses that from somatostatin (SOM)-positive interneurons. (a) Left: experimental scheme. Stimulation of dmPFC with blue light and recording from principal neurons in layer V are illustrated. Right: fluorescent microscope images of ChR2-YFP expressed in PV and SOM interneurons in dorso-medial prefrontal cortex (dmPFC) shown at low and high magnifications. The corresponding areas are marked by white rectangles. (b) Left: examples of IPSCs evoked in the same cells by 5 Hz train of blue light stimulation of PV-interneurons expressing ChR2 before and after perfusion with CGP52432 (10 μM), averages of five sweeps are shown. Arrowheads under each sweep show the time of stimulation. Middle: amplitudes of the first IPSCs in the train before and after perfusion with CGP52432, lines connect data points representing the same cells. Right: IPSCs amplitudes and time integrals normalized to the values of the first IPSC, before and after perfusion with CGP52432. Black and gray colors represent control (16 cells/3 mice) and OF (16 cells/3 mice) groups, respectively. (c) Same experiment as in (b), except ChR2, was expressed in SOM-INs. Control: 11 cells/3 mice, OF: 10 cells/3 mice. ASCF *vs* CGP52432: $*p<0.05$, $**p<0.01$, and $***p<0.001$. Error bars represent SEM.

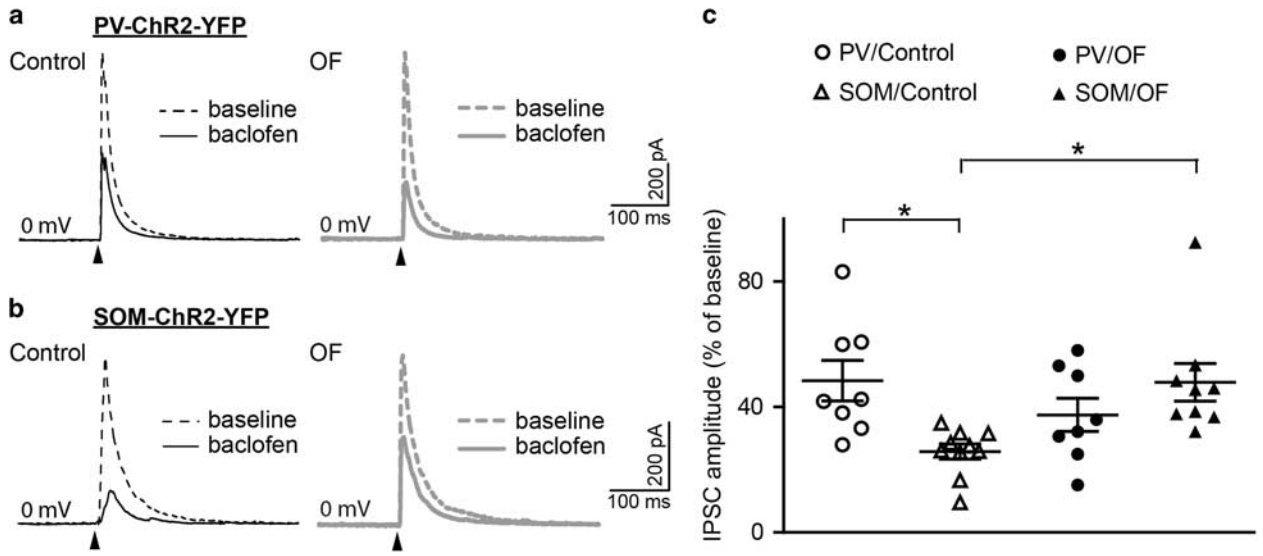

Figure 6 Observational fear training (OF) decreases sensitivity to baclofen in somatostatin (SOM) interneurons, but not in parvalbumin (PV) interneurons. (a) Examples of inhibitory postsynaptic currents (IPSCs) evoked in dorso-medial prefrontal cortex (dmPFC) principal neurons by a single pulse of blue light stimulation of PV-interneurons expressing ChR2, before (Baseline, dashed lines) and after 5 min exposure to 20 μM baclofen in the bath (Baclofen, continuous lines) in control (Control: eight cells/three mice) and OF (eight cells/three mice) groups. Averages of 10 sweeps are shown. Arrowheads under each sweep show the time of blue light stimulation. (b) Same as in a for blue light stimulation of SOM interneurons expressing ChR2. Control: 10 cells/3 mice; OF: 9 cells/3 mice. (c) Summary diagram for amplitudes of IPSCs in the presence of baclofen as % of values before baclofen perfusion. *$p<0.05$. Error bars represent SEM.

(Figure 4d), which suggests that GABAbR also mediates effects of OF on the dynamics of evoked IPSC originating from distal dendrites.

OF Training has Opposing Effects on Inputs from PV- and SOM-INs

Inhibitory inputs in soma and distal dendrites of cortical neurons are preferentially formed by the PV and SOM interneurons, respectively (Freund and Buzsaki, 1996; Markram *et al*, 2004; Petilla Interneuron Nomenclature *et al*, 2008). To examine effects of OF on these inputs and role of GABAb receptors, we recorded IPSCs evoked in the layer V PCs by blue light stimulation of either PV-INs (PV-IPSCs) or SOM-INs (SOM-IPSCs) expressing channelrhodopsin-2 (Figure 5a). IPSCs from the same neurons were recorded in the absence and then in the presence of CGP52432, which did not change the amplitude of the first SOM-IPSCs and PV-IPSCs in the trains (Figures 5b and c, middle).

The PV-IPSC amplitudes and charge transfer decreased along the train in both control and OF groups (amplitude: control, $F(4,15)=111$, $p<0.0001$; OF, $F(4,15)=221$, $p<0.0001$; charge transfer: control, $F(4,15)=166$, $p<0.0001$; OF, $F(4,15)=222$, $p<0.0001$, repeated measure ANOVA), but the IPSC depression was stronger in OF group than in controls (behavioral treatment*amplitude interaction: $F(4,30)=12.5$, $p<0.0001$; behavioral treatment*charge transfer interaction $F(4,30)=8.2$, $p<0.0001$). CGP52432 had no significant effect on IPSC depression in controls (CGP52432*IPSC amplitude interaction: $F(4,30)=0.35$, $p=0.84$; CGP52432*IPSC charge interaction $F(4,30)=0.17$, $p=0.95$), but attenuated IPSC depression in the OF group (CGP52432*IPSC amplitude interaction: $F(4,30)=9.1$, $p<0.0001$; CGP52432*IPSC charge interaction $F(4,30)=4.1$, $p=0.004$) (Figure 5b right), thereby eliminating the differences between the control and OF groups in IPSC dynamics (behavioral treatment*amplitude interaction: $F(4,30)=1.0$, $p=0.4$; behavioral treatment*charge transfer interaction $F(4,30)=0.6$, $p=0.7$).

The SOM-IPSC amplitudes and charge transfers also decreased along the train in both control and OF groups (amplitude: control, $F(4,10)=121$, $p<0.0001$; OF, $F(4,9)=38$, $p<0.0001$; charge transfer: control, $F(4,10)=127$, $p<0.0001$; OF, $F(4,9)=103$, $p<0.0001$, repeated measure ANOVA); however, in contrast to its effect on PV-IPSCs, OF attenuated the depression of SOM-IPSC (behavioral treatment*amplitude interaction: $F(4,19)=12.9$, $p<0.0001$; behavioral treatment*charge transfer interaction $F(4,19)=16$, $p<0.0001$). CGP52432 attenuated SOM-IPSC depression in both, the control and OF groups (control, CGP52432*IPSC amplitude interaction: $F(4,20)=39$, $p<0.0001$; CGP52432*IPSC charge interaction $F(4,20)=24$, $p<0.0001$; OF, CGP52432*IPSC amplitude interaction: $F(4,18)=5.9$, $p=0.0004$; and CGP52432*IPSC charge interaction: $F(4,18)=209$, $p<0.0001$) (Figure 5c right), eliminating the differences between the groups in IPSC dynamics (behavioral treatment*amplitude interaction: $F(4,19)=1.2$, $p=0.32$; behavioral treatment*charge transfer interaction $F(4,19)=1.8$, $p=0.14$). These results suggested that GABAbR mediates effects of OF on the dynamics of evoked IPSCs from PV- and SOM-INs in the opposing manners.

OF Training has a Different Effect on GABAbR Control of GABA Release from SOM- than PV-INs

To quantify GABAbR-mediated inhibition of GABA release in inputs to the layer V PCs from PV and SOM neurons, we examined effects of a GABAbR agonist baclofen on PV-IPSCs and SOM-IPSCs either in controls or OF cells.

Five-minute perfusion with 20 μM baclofen significantly inhibited IPSCs in all four experimental groups (IPSC amplitude % of baseline compared to 100, $p<0.0001$) (Figure 6). One-way AVONA revealed significant differences among the four groups ($p<0.01$). Bonferroni's multiple comparisons revealed significant differences between the PV/Control and SOM/Control ($p<0.05$), between SOM/Control and SOM/OF ($p<0.05$), but not between PV/Control and PV/OF groups. Two-way ANOVA revealed a significant 'IPSC type'*'behavioral treatment' interaction ($p<0.01$) and Bonferroni posttest showed a significant effect of behavioral treatment on the SOM-IPSCs ($p<0.01$), but not on the PV-IPSCs. Thus, under control conditions, GABAbR exerts stronger inhibition of GABA release from SOM-INs than from PV-INs but OF eliminates that difference by attenuating GABAbR suppression of GABA release from SOM-INs.

DISCUSSION

The key finding here is that the OF, one form of purely emotional distress in mice, reorganizes inhibition of dmPFC layer V pyramidal neurons by attenuating the GABAbR control of GABA release from SOM-INs, but not from PV-INs, which underlie mainly dendritic and somatic inhibition, respectively. This study, however, does not rule out a possibility of such changes on exposure to other stressors. Furthermore, it remains to be determined whether the observed changes could be attributed to the contextual learning during OF (Jeon *et al*, 2010) or to the effect of trauma on future learning in the PA paradigm (Ito *et al*, 2015).

Imaging studies have demonstrated that traumatic events alter functional connectivity of the prefrontal cortex in humans (Krause-Utz *et al*, 2014; Lanius *et al*, 2010; Long *et al*, 2014; van Wingen *et al*, 2012) and rodents (Henckens *et al*, 2015; Liang *et al*, 2014), but synaptic process underlying such changes remains largely unexplored. To that end, we examined OF-induced synaptic adaptations in PCs in dmPFC layer V, which are one of the major outputs of dmPFC. These cells can serve as a reporter of alterations in multiple microcircuits within dmPFC, because their dendrites span through all cortical layers and integrate inputs from remote and local afferents. We electrically stimulated dmPFC layer I, which contains axons arriving from cortex and thalamus, as well as local ascending glutamatergic and GABAergic axons. The 5 Hz stimulation frequency was selected as physiologically relevant, given the 'midline frontal theta' 3-7 Hz band correlation with working memory in humans (Gevins *et al*, 1997; Sauseng *et al*, 2010) and the predominance of the 2-5 Hz band in PFC of the rat (Fujisawa and Buzsaki, 2011).

Dynamics of Excitation and Inhibition

OF increased the likelihood of action potentials in PCs during the 5 Hz stimulation train, which was consistent with the emerged EPSP facilitation along that train. The EPSP facilitation was no longer seen in the presence of GABAa receptor blocker picrotoxin, which indicated that GABAergic transmission was essential for that facilitation. The stronger decline of evoked inhibition along the train may underlie the observed EPSP facilitation after OF.

The Role of GABAbR

Presynaptic GABAbR mediates short-term depression of GABAergic synapses during repeated stimulation in the somatosensory and insular cortex, particularly when the interval between stimuli is within 150–300 ms (Fukuda *et al*, 1993; Kobayashi *et al*, 2012). Surprisingly, in our preparation in the control group, a GABAbR blocker CGP52432 had no significant effect on IPSC depression. However, in the OF group, CGP52432 decreased the depression, thus abolishing effects of OF. It indicates that OF recruits GABAbR to enhance the IPSC depression, which is normally GABAbR independent. The observed effects of CGP52432 on IPSCs are unlikely to involve postsynaptic GABAbR, because QX314, which blocks GABAbR-mediated hyperpolarization (Andrade, 1991; McLean *et al*, 1996; Nathan *et al*, 1990), was included in the internal solution.

In the analyses of evoked excitation in the layer 5 principal cells, CGP52432 eliminated the differences between the OF and control groups in both firing and EPSP dynamics, which suggests that GABAbR is contributing to the effects of OF on evoked excitation. This contribution could involve GABAbR both in principal cells in interneurons because bath applied CGP52432 blocks GABAbR in all cells.

Somatic *vs* Dendritic Inhibition

Given that somatic voltage clamp poorly controls voltage at distal dendrites (Williams and Mitchell, 2008), the somatically recorded IPSCs mainly represent synaptic events near the soma and can be considered as 'somatically enriched IPSCs'. Then, we enriched recordings for IPSCs originating from distal dendrites by puffing picrotoxin on the soma of recorded neurons. The properties of the 'dendritically enriched IPSCs' were different from those of the somatically enriched IPSCs. First, in the control group, they exhibited stronger depression, which was sensitive to CGP52432. Second, OF training rather attenuated their depression and decreased its sensitivity to CGP52432. These results indicate that OF attenuates GABAbR control over GABAergic inputs to distal dendrites, which is normally stronger than over inputs to soma. Through these opposing effects on GABAbR control of somatic *vs* dendritic IPSC, OF training may equalize the dynamics of IPSC depression along the somatodendritic axis. Yet, our analysis does not distinguish between IPSCs originating at the soma vs proximal dendrites, because it remains unclear at what distance from the soma picrotoxin puff was blocking GABAa receptor.

GABAbR-Dependent Alterations in PV-IN and SOM-IN Inputs to L5 PCs

To identify cells that underlie the observed GABAbR control of GABA transmission, IPSCs originating from PV- and SOM-INs (PV-IPSCs and SOM-IPSCs, respectively) were isolated by blue light stimulation of interneurons expressing ChR2. The effects of OF training and GABAbR blocker CGP52432 on PV-IPSCs were very similar with their effects on 'somatically enriched' IPSCs evoked by electrical stimulation of dmPFC layer 1 in the absence of picrotoxin puff. Conversely, effects on SOM-IPSCs resembled those on 'dendritically enriched' IPSCs, which were evoked by the

same electrical stimulation, but after picrotoxin puff to soma. Although electrical stimulation differs from the blue light stimulation by recruiting broader neuronal networks including several types of SOM-negative INs, such as the 5-HT receptor 3 expressing cells that target distal dendrites, and also GABAergic synapses between INs, such as the strong inputs from SOM-INs to PV-INs (Marlin and Carter, 2014; Pfeffer *et al*, 2013), these observations indicate that picrotoxin puffs to the soma successfully shift the origin of recorded IPSCs from the soma to distal dendrites, consistent with the preferential targeting of PC soma by PV-INs and distal dendrites by SOM-INs, respectively (Freund and Buzsaki, 1996; Markram *et al*, 2004; Petilla Interneuron Nomenclature *et al*, 2008).

The strong modulation by GABAbR appears to be a distinct property of SOM-INs. In controls, CGP52432 strongly attenuated the depression of SOM-IPSCs (Figure 4c), but barely affected the depression of PV-IPSCs (Figure 4b), indicating that GABAbR control of SOM-INs is stronger than of PV-INs. This was consistent with the greater sensitivity to baclofen of the SOM-IPSCs than the PV-IPSCs in control mice, suggesting that SOM-INs naturally express more functional GABAbR, which agrees with an earlier finding in the hippocampus that SOM-INs have stronger GABAbR1 immunoreactivity than all other cells (Sloviter *et al*, 1999). The cell-type specific differences in GABAbR function could be an adaptation to possibly different local concentrations of GABA, high at perisomatic basket-type synapses and low at sparse dendritic synapses.

The attenuation of GABAbR-mediated depression of SOM-IPSCs after OF training is readily explained by decreased GABAbR function in SOM-INs, detected as decreased sensitivity of SOM-IPSCs to baclofen (Figure 5). Paradoxically, despite OF training enhanced the GABAbR-mediated depression of PV-IPSCs, there was only a trend towards higher sensitivity of PV-IPSCs to baclofen. This discrepancy may reflect distinct modulation of GABAbR in each subcellular domain: the 5 Hz stimulation is expected to activate GABAbRs mostly near GABAergic terminals; whereas bath applied baclofen activates all receptors including those on soma and dendrites. The somatic and dendritic receptors can attenuate GABA release by preventing action potentials and thereby mask the effect from GABAbR upregulation at terminals after OF training.

The finding of altered GABAbR function one day after OF indicates long-term changes in either the receptor or its downstream targets. The possible mechanisms may involve NMDA receptor, which often participates in long-lasting plastic changes and has been shown to control trafficking and surface expression of GABAbR via the CaMKII–AMPK phosphorylation cascade (Guetg *et al*, 2010; Maier *et al*, 2010; Terunuma *et al*, 2010). Changing GABAbR kinetics properties by the KCTD family of axillary proteins (Gassmann and Bettler, 2012; Schwenk *et al*, 2010) or modulation via several recently discovered interacting proteins (Schwenk *et al*, 2016) may also be involved. Some of these mechanisms have been documented in dendrites of glutamatergic neurons but remain to be tested in GABAergic terminals. Understanding what underlies opposing regulation of GABAbR in PV- and SOM-INs may reveal the individual role of these cells during brain response to stress.

Rerouting Information Flows in dmPFC as a Possible Functional Implication

We found OF to rebalance inhibitory drive along the somatodendritic axis by changing GABAbR function in opposing ways in PV-INs for perisomatic inhibition and in SOM-INs for dendritic inhibition. As GABA transmission competes with glutamatergic inputs at dendrites by suppressing calcium spike (Perez-Garci *et al*, 2006) and local dendritic depolarization, which determines the direction of synaptic plasticity towards LTP or LTD (Sjostrom and Hausser, 2006), the OF training may reroute information flow across dmPFC by attenuating glutamatergic inputs to distal parts of dendrites, but enhancing inputs to soma and proximal dendrites. For intra-dmPFC communication, OF is expected to enhance connectivity among L5 PCs, because they receive inputs from one another mainly in the proximal basal dendritic tree (Markram *et al*, 1997), but to weaken those connections of layer 2/3 neurons, which synapse on apical dendrites of layer 5 PCs (Thomson and Bannister, 1998). For the remote connectivity, OF is expected to attenuate corticocortical and thalamocortical inputs that target layer I of dmPFC, but to strengthen communication with areas such as the hippocampus and basolateral amygdala that send abundant projections to the deep layers (Cruikshank *et al*, 2010; Hoover and Vertes, 2007; Jay and Witter, 1991; Oh *et al*, 2014). The consequences can be even more interesting and complex. Studies in the hippocampus revealed that during synchronous activity, different classes of INs exhibit different firing patterns during different behavioral states and associated forms of oscillations (Klausberger *et al*, 2003). Furthermore, INs targeting different subcellular domains fire at different phases of the oscillation cycle (Klausberger and Somogyi, 2008), which was proposed to cause temporal redistribution of inhibition along the somatodendritic axis of PCs and thereby to maintain or segregate cell assemblies (Somogyi *et al*, 2014). By modifying that process, OF may contribute to either formation or dissolution of cell assemblies between L5 PC and remote neurons, depending on the somatodendritic location of their inputs to L5 PCs, and also, on the behavioral state and the corresponding pattern of oscillatory activity.

FUNDING AND DISCLOSURE

The authors declare no conflict of interest.

ACKNOWLEDGMENTS

This research was supported by VTCRI, Whitehall Foundation and NIMH grant R21MH112093.

REFERENCES

Andrade R (1991). Blockade of neurotransmitter-activated K+ conductance by QX-314 in the rat hippocampus. *Eur J Pharmacol* **199**: 259–262.

Bero AW, Meng J, Cho S, Shen AH, Canter RG, Ericsson M *et al* (2014). Early remodeling of the neocortex upon episodic memory encoding. *Proc Natl Acad Sci USA* **111**: 11852–11857.

Chen Q, Panksepp JB, Lahvis GP (2009). Empathy is moderated by genetic background in mice. *PLoS ONE* **4**: e4387.

Cougle JR, Resnick H, Kilpatrick DG (2009). Does prior exposure to interpersonal violence increase risk of PTSD following subsequent exposure? *Behav Res Ther* **47**: 1012–1017.

Cruikshank SJ, Urabe H, Nurmikko AV, Connors BW (2010). Pathway-specific feedforward circuits between thalamus and neocortex revealed by selective optical stimulation of axons. *Neuron* **65**: 230–245.

Freund TF, Buzsaki G (1996). Interneurons of the hippocampus. *Hippocampus* **6**: 347–470.

Fujisawa S, Buzsaki G (2011). A 4 Hz oscillation adaptively synchronizes prefrontal, VTA, and hippocampal activities. *Neuron* **72**: 153–165.

Fukuda A, Mody I, Prince DA (1993). Differential ontogenesis of presynaptic and postsynaptic GABAB inhibition in rat somatosensory cortex. *J Neurophysiol* **70**: 448–452.

Gabbott PL, Warner TA, Jays PR, Salway P, Busby SJ (2005). Prefrontal cortex in the rat: projections to subcortical autonomic, motor, and limbic centers. *J Compar Neurol* **492**: 145–177.

Gassmann M, Bettler B (2012). Regulation of neuronal GABA(B) receptor functions by subunit composition. *Nat Rev Neurosci* **13**: 380–394.

Gevins A, Smith ME, McEvoy L, Yu D (1997). High-resolution EEG mapping of cortical activation related to working memory: effects of task difficulty, type of processing, and practice. *Cereb Cortex* **7**: 374–385.

Guetg N, Abdel Aziz S, Holbro N, Turecek R, Rose T, Seddik R *et al* (2010). NMDA receptor-dependent GABAB receptor internalization via CaMKII phosphorylation of serine 867 in GABAB1. *Proc Natl Acad Sci USA* **107**: 13924–13929.

Henckens MJ, van der Marel K, van der Toorn A, Pillai AG, Fernandez G, Dijkhuizen RM *et al* (2015). Stress-induced alterations in large-scale functional networks of the rodent brain. *Neuroimage* **105**: 312–322.

Hippenmeyer S, Vrieseling E, Sigrist M, Portmann T, Laengle C, Ladle DR *et al* (2005). A developmental switch in the response of DRG neurons to ETS transcription factor signaling. *PLoS Biol* **3**: e159.

Hirai Y, Morishima M, Karube F, Kawaguchi Y (2012). Specialized cortical subnetworks differentially connect frontal cortex to parahippocampal areas. *J Neurosci* **32**: 1898–1913.

Hoover WB, Vertes RP (2007). Anatomical analysis of afferent projections to the medial prefrontal cortex in the rat. *Brain Struct Funct* **212**: 149–179.

Ito W, Erisir A, Morozov A (2015). Observation of distressed conspecific as a model of emotional trauma generates silent synapses in the prefrontal-amygdala pathway and enhances fear learning, but ketamine abolishes those effects. *Neuropsychopharmacology* **40**: 2536–2545.

Jay TM, Witter MP (1991). Distribution of hippocampal CA1 and subicular efferents in the prefrontal cortex of the rat studied by means of anterograde transport of Phaseolus vulgaris-leucoagglutinin. *J Compar Neurol* **313**: 574–586.

Jeon D, Kim S, Chetana M, Jo D, Ruley HE, Lin SY *et al* (2010). Observational fear learning involves affective pain system and Cav1.2 Ca2+ channels in ACC. *Nat Neurosci* **13**: 482–488.

Kim D, Jeong H, Lee J, Ghim JW, Her ES, Lee SH *et al* (2016). Distinct roles of parvalbumin- and somatostatin-expressing interneurons in working memory. *Neuron* **92**: 902–915.

Klausberger T, Magill PJ, Marton LF, Roberts JD, Cobden PM, Buzsaki G *et al* (2003). Brain-state- and cell-type-specific firing of hippocampal interneurons in vivo. *Nature* **421**: 844–848.

Klausberger T, Somogyi P (2008). Neuronal diversity and temporal dynamics: the unity of hippocampal circuit operations. *Science* **321**: 53–57.

Kobayashi M, Takei H, Yamamoto K, Hatanaka H, Koshikawa N (2012). Kinetics of GABAB autoreceptor-mediated suppression of GABA release in rat insular cortex. *J Neurophysiol* **107**: 1431–1442.

Krause-Utz A, Elzinga BM, Oei NY, Paret C, Niedtfeld I, Spinhoven P *et al* (2014). Amygdala and dorsal anterior cingulate connectivity during an emotional working memory task in borderline personality disorder patients with interpersonal trauma history. *Front Hum Neurosci* **8**: 848.

Lanius RA, Bluhm RL, Coupland NJ, Hegadoren KM, Rowe B, Theberge J *et al* (2010). Default mode network connectivity as a predictor of post-traumatic stress disorder symptom severity in acutely traumatized subjects. *Acta Psych Scand* **121**: 33–40.

Liang Z, King J, Zhang N (2014). Neuroplasticity to a single-episode traumatic stress revealed by resting-state fMRI in awake rats. *Neuroimage* **103**: 485–491.

Long J, Huang X, Liao Y, Hu X, Hu J, Lui S *et al* (2014). Prediction of post-earthquake depressive and anxiety symptoms: a longitudinal resting-state fMRI study. *Sci Rep* **4**: 6423.

Maier PJ, Marin I, Grampp T, Sommer A, Benke D (2010). Sustained glutamate receptor activation down-regulates GABAB receptors by shifting the balance from recycling to lysosomal degradation. *J Biol Chem* **285**: 35606–35614.

Malin EL, Ibrahim DY, Tu JW, McGaugh JL (2007). Involvement of the rostral anterior cingulate cortex in consolidation of inhibitory avoidance memory: interaction with the basolateral amygdala. *Neurobiol Learn Mem* **87**: 295–302.

Malin EL, McGaugh JL (2006). Differential involvement of the hippocampus, anterior cingulate cortex, and basolateral amygdala in memory for context and footshock. *Proc Natl Acad Sci USA* **103**: 1959–1963.

Markram H, Lubke J, Frotscher M, Roth A, Sakmann B (1997). Physiology and anatomy of synaptic connections between thick tufted pyramidal neurones in the developing rat neocortex. *J Physiol* **500**(Pt 2): 409–440.

Markram H, Toledo-Rodriguez M, Wang Y, Gupta A, Silberberg G, Wu C (2004). Interneurons of the neocortical inhibitory system. *Nat Rev Neurosci* **5**: 793–807.

Marlin JJ, Carter AG (2014). GABA-A receptor inhibition of local calcium signaling in spines and dendrites. *J Neurosci* **34**: 15898–15911.

McLean HA, Caillard O, Khazipov R, Ben-Ari Y, Gaiarsa JL (1996). Spontaneous release of GABA activates GABAB receptors and controls network activity in the neonatal rat hippocampus. *J Neurophysiol* **76**: 1036–1046.

Nathan T, Jensen MS, Lambert JD (1990). The slow inhibitory postsynaptic potential in rat hippocampal CA1 neurones is blocked by intracellular injection of QX-314. *Neurosci Lett* **110**: 309–313.

Oh SW, Harris JA, Ng L, Winslow B, Cain N, Mihalas S *et al* (2014). A mesoscale connectome of the mouse brain. *Nature* **508**: 207–214.

Perez-Garci E, Gassmann M, Bettler B, Larkum ME (2006). The GABAB1b isoform mediates long-lasting inhibition of dendritic Ca2+ spikes in layer 5 somatosensory pyramidal neurons. *Neuron* **50**: 603–616.

Petilla Interneuron Nomenclature G, Ascoli GA, Alonso-Nanclares L, Anderson SA, Barrionuevo G, Benavides-Piccione R *et al* (2008). Petilla terminology: nomenclature of features of GABAergic interneurons of the cerebral cortex. *Nat Rev Neurosci* **9**: 557–568.

Pfeffer CK, Xue M, He M, Huang ZJ, Scanziani M (2013). Inhibition of inhibition in visual cortex: the logic of connections between molecularly distinct interneurons. *Nat Neurosci* **16**: 1068–1076.

Ramaswamy S, Markram H (2015). Anatomy and physiology of the thick-tufted layer 5 pyramidal neuron. *Front Cell Neurosci* **9**: 233.

Resnick HS, Yehuda R, Pitman RK, Foy DW (1995). Effect of previous trauma on acute plasma cortisol level following rape. *Am J Psychiatry* **152**: 1675–1677.

Sauseng P, Griesmayr B, Freunberger R, Klimesch W (2010). Control mechanisms in working memory: a possible function of EEG theta oscillations. *Neurosci Biobehav Rev* **34**: 1015–1022.

Schwenk J, Metz M, Zolles G, Turecek R, Fritzius T, Bildl W *et al* (2010). Native GABA(B) receptors are heteromultimers with a family of auxiliary subunits. *Nature* **465**: 231–235.

Schwenk J, Perez-Garci E, Schneider A, Kollewe A, Gauthier-Kemper A, Fritzius T *et al* (2016). Modular composition and dynamics of native GABAB receptors identified by high-resolution proteomics. *Nat Neurosci* **19**: 233–242.

Shepherd GM (2013). Corticostriatal connectivity and its role in disease. *Nat Rev Neurosci* **14**: 278–291.

Sjostrom PJ, Hausser M (2006). A cooperative switch determines the sign of synaptic plasticity in distal dendrites of neocortical pyramidal neurons. *Neuron* **51**: 227–238.

Sloviter RS, Ali-Akbarian L, Elliott RC, Bowery BJ, Bowery NG (1999). Localization of GABA(B) (R1) receptors in the rat hippocampus by immunocytochemistry and high resolution autoradiography, with specific reference to its localization in identified hippocampal interneuron subpopulations. *Neuropharmacology* **38**: 1707–1721.

Sohal VS, Zhang F, Yizhar O, Deisseroth K (2009). Parvalbumin neurons and gamma rhythms enhance cortical circuit performance. *Nature* **459**: 698–702.

Somogyi P, Katona L, Klausberger T, Lasztoczi B, Viney TJ (2014). Temporal redistribution of inhibition over neuronal subcellular domains underlies state-dependent rhythmic change of excitability in the hippocampus. *Phil Trans R Soc Lond Ser B Biol Sci* **369**: 20120518.

Taniguchi H, He M, Wu P, Kim S, Paik R, Sugino K *et al* (2011). A resource of Cre driver lines for genetic targeting of GABAergic neurons in cerebral cortex. *Neuron* **71**: 995–1013.

Terunuma M, Vargas KJ, Wilkins ME, Ramirez OA, Jaureguiberry-Bravo M, Pangalos MN *et al* (2010). Prolonged activation of NMDA receptors promotes dephosphorylation and alters post-endocytic sorting of GABAB receptors. *Proc Natl Acad Sci USA* **107**: 13918–13923.

Thomson AM, Bannister AP (1998). Postsynaptic pyramidal target selection by descending layer III pyramidal axons: dual intracellular recordings and biocytin filling in slices of rat neocortex. *Neuroscience* **84**: 669–683.

van Wingen GA, Geuze E, Vermetten E, Fernandez G (2012). The neural consequences of combat stress: long-term follow-up. *Mol Psychiatry* **17**: 116–118.

Williams SR, Mitchell SJ (2008). Direct measurement of somatic voltage clamp errors in central neurons. *Nat Neurosci* **11**: 790–798.

Yusufishaq S, Rosenkranz JA (2013). Post-weaning social isolation impairs observational fear conditioning. *Behav Brain Res* **242**: 142–149.